Available online at www.sciencedirect.com
ScienceDirect
International Journal of Heat and Mass Transfer 50 (2007) 2339–2345
International Journal of HEAT and MASS TRANSFER
www.elsevier.com/locate/ijhmt

Flow boiling heat transfer characteristics of nitrogen in plain and wire coil inserted tubes

Rin Yun [a], Jee-Sang Hwang [b], Jin Tack Chung [b], Yongchan Kim [b,*]

[a] Department of Mechanical Engineering, Hanbat National University, Duckmyung-dong, Yuseong-ku, Daejeon 305-719, Republic of Korea
[b] Department of Mechanical Engineering, Korea University, Anam-dong, Sungbuk-ku, Seoul 136-701, Republic of Korea

Received 15 March 2006; received in revised form 21 October 2006
Available online 28 December 2006

Abstract

Boiling heat transfer characteristics of nitrogen were experimentally investigated in a stainless steel plain tube and wire coil inserted tubes. Wire coils having different coil pitches and wire thicknesses were inserted into a horizontally positioned plain tube, which had an inner diameter of 10.6 mm and a length of 1.65 m. The coil pitches were 18.4, 27.6, and 36.8 mm, and the wire thicknesses were 1.5, 2.0, and 2.5 mm. Tests were conducted at a saturation temperature of −191 °C, mass fluxes from 58 to 105 kg/m^2 s, and heat fluxes from 22.5 to 32.7 kW/m^2. A direct heating method was used to apply heat to the test tube. The boiling heat transfer coefficients of nitrogen significantly decreased when the dryout occurred. Enhancement performance ratio (EPR), which is the ratio of heat transfer enhancement factor to pressure drop ratio, was used to evaluate the performance of the wire coil inserts. The maximum heat transfer enhancement of the wire coil inserted tubes over the plain tube was 174% with wire 3 having a twist ratio (p/D_w) of 1.84 and a thickness ratio (t/D_w) of 0.25. Wire 3-inserted tube showed the highest EPR among the tested tubes in this study.

Keywords: Boiling heat transfer; Wire coil; Nitrogen; Dryout; EPR

1. Introduction

Flow boiling heat transfer and pressure drop characteristics of cryogenic fluids are very important in the design of cryogenic systems, such as a LNG (liquefied natural gas) vaporizer, cryogenic fluid storage vessels, air separation systems, and aerospace systems. Generally, the boiling heat transfer characteristics of cryogenic fluids are much different from those of conventional refrigerants in terms of the early dryout of liquid film and film boiling [1–4]. When liquid film dryout or film boiling occurs, the boiling heat transfer coefficients decrease dramatically from the values at the pre-dryout conditions. Therefore, in order to increase the performance of the LNG vaporizer, it is essential to enhance the boiling heat transfer coefficient of cryogenic fluids in its tubes.

Under the dryout and film boiling conditions, twisted-tape inserts, wire coil inserts, and internally finned tubes were used to increase the boiling heat transfer coefficients. Mori et al. [5] investigated the effects of twisted-tape inserts and wire coil inserts on the boiling heat transfer and pressure drop characteristics of LNG. When the twisted-tape and the wire coil were inserted to a plain tube, the boiling heat transfer coefficients increased by 100–280% more than that of the plain tube at a mass flux of 88 kg/m^2 s. Nam et al. [6] studied the effects of wire coil inserts on the boiling heat transfer characteristics of nitrogen. The boiling heat transfer coefficients of the wire coil inserted tube were higher than those of a plain tube by 170–200%. Bergles et al. [7] investigated the effects of swirl flow induced by a twisted-tape on the dispersed flow film boiling of nitrogen. They reported that the swirl flow enhanced the heat transfer coefficients and thermal non-equilibrium.

Even though several research studies were conducted on the boiling heat transfer characteristics in wire coil inserted

* Corresponding author. Tel.: +82 2 3290 3364; fax: +82 2 921 5439.
E-mail address: yongckim@korea.ac.kr (Y. Kim).

0017-9310/$ - see front matter © 2006 Elsevier Ltd. All rights reserved.
doi:10.1016/j.ijheatmasstransfer.2006.10.038

Nomenclature

A	tube inside area, m^2
D	tube diameter, mm
EF	enhancement factor
EPR	enhancement performance ratio
G	mass flux, kg/m^2 s
h	heat transfer coefficient, W/m^2 K
i	enthalpy, kJ/kg
l	tube length, m
$\dot{m}$	mass flow rate, kg/s
PDR	pressure drop ratio
p	coil pitch, mm
Q	heat transfer rate, kW
q''	heat flux, kW/m^2
Re	Reynolds number
T	temperature, K
t	wire thickness, mm
x	vapor quality
z	direction of tube length

Greek symbols

Δi_{lv}	latent heat of vaporization per unit mass, kJ/kg
ΔP	pressure drop, kPa
ρ	density, kg/m^3

Subscripts

en	enhancement
f	fluid
i	inner
in	inlet
l	liquid
out	outlet
v	vapor
w	wall, wire

tubes, very few studies were focused on the effects of wire coil geometries, such as coil pitch and wire thickness. In addition, the effects of vapor quality were rarely reported in literature. This study investigates the boiling heat transfer and pressure drop characteristics of nitrogen in a plain tube and wire coil inserted tubes. Especially, this study represents the effects of wire coil inserts on heat transfer characteristics of nitrogen with a variation of coil pitch and wire thickness. EPR, which is the ratio of heat transfer enhancement factor to pressure drop ratio, was used to evaluate the performance of the wire coil inserts.

2. Experimental setup

2.1. Test setup and instrumentation

Fig. 1 shows the experimental setup. A liquid nitrogen tank, a test tube, a DC power supply, and post-heaters were used. During the tests, the pressure inside the nitrogen tank was maintained at 1.5–2.0 MPa. The outlet of the test section was exposed to atmosphere. The pressure difference between the nitrogen tank and ambient forced nitrogen circulated into the test section. The flow rate of nitrogen was controlled by using an adjustable needle valve. Heat was added into the test tube by the direct heating method using the DC power supply. A safety valve was installed at the exit of the test tube to handle abrupt expansion of liquid nitrogen. Post-heaters were used to increase the nitrogen temperature to ambient temperature, which is a crucial process for safe operation and for a volumetric flow meter working at ambient temperature. Until the nitrogen temperature reached ambient temperature at the outlet of the test section, the nitrogen was discharged through the bypass line without passing through the volumetric flow meter (Fig. 1).

Fig. 2 shows the details of the test tube. The test tube, which was made of stainless steel, had inner diameter of 10.6 mm and a length of 1.65 m. Four T-type thermocouple probes were installed at the inlet and exit of the test tube, the exit of the post-heaters, and the inlet of the volumetric flow meter, respectively. Thermocouples were evenly installed along the test tube at five positions to measure surface temperatures. At each position, two thermocouples, which were electrically insulated by thin Teflon tape, were attached at the bottom and the top side of the test tube. To minimize the heat gain from the ambient, a vacuum insulation was used on the outside of the test tube. Dielectric and Teflon fittings across the test tube prevented any electric leakage due to the DC power supply.

All thermocouples were calibrated by using a precision thermometer with an accuracy of ±0.1 °C. Pressure transducers were installed at the inlet of the test tube and the inlet of the volumetric flow meter. The measurement range and the accuracy of the pressure transducers were 0–250 psig and ±0.13% of the full scale, respectively. A differential pressure transducer was installed to measure the pressure drop across the test tube. The range and the accuracy of the differential pressure transducer were 0–25 psid and ±0.5% of full scale, respectively. The range and accuracy of the volumetric flow meter were 60–600 LPM and ±3%, respectively. The estimated uncertainties of the heat transfer coefficients were less than 5.7%.

Fig. 3 and Table 1 show the geometries and specifications of the wire coil inserts, respectively. The coil diameter was 10.0 mm, and the twist ratio, p/D_w, varied at 1.84, 2.76, and 3.68. The thickness ratios, t/D_w, were 0.15, 0.2, and 0.25.

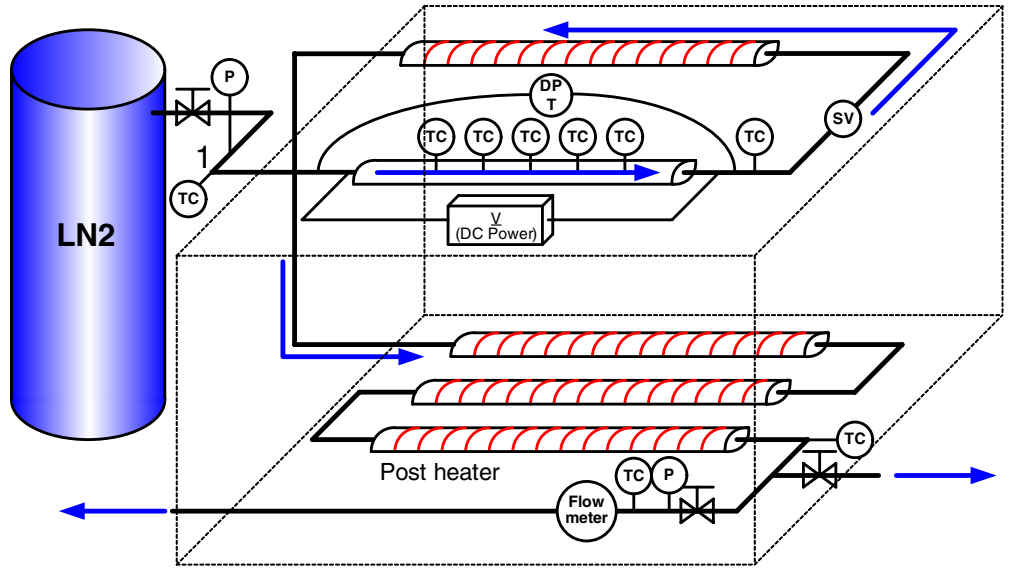

Fig. 1. Schematic of the experimental setup.

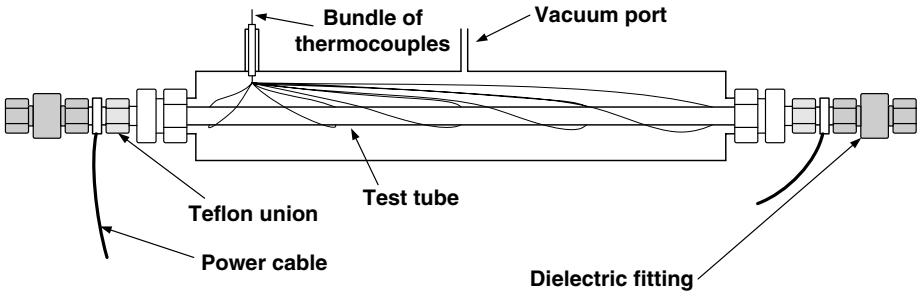

Fig. 2. Details of the test section.

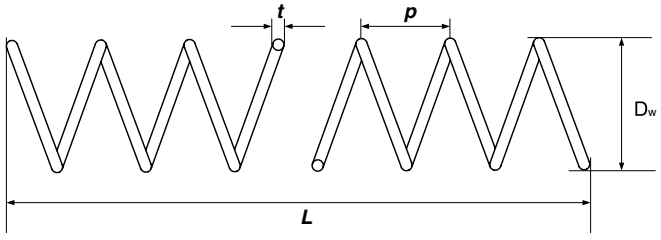

Fig. 3. Geometries of wire coil inserts.

2.2. Test conditions and data reduction

The tests were conducted at a saturation temperature of −191 °C, mass fluxes from 58 to 105 kg/m^2 s, and heat fluxes from 22.5 to 32.7 kW/m^2.

Estimating the exact heat input to the test tube was crucial in the present experiments because even a small amount of heat gain from the ambient can cause large deviations in the determination of the nitrogen state. In order to estimate the heat gain precisely, the nitrogen exiting the storage tank was maintained at subcooled liquid state, and the outlet condition of the test tube was set to

Table 1
Specification of wire coil inserts

Wire coil no.	Tube inner diameter, D_i (mm)	Coil diameter, D_w (mm)	Wire thickness, t (mm)	Coil pitch, p (mm)	t/D_w	p/D_w
Wire 1	10.6	10.0	1.5	18.4	0.15	1.84
Wire 2	10.6	10.0	2.0	18.4	0.20	1.84
Wire 3	10.6	10.0	2.5	18.4	0.25	1.84
Wire 4	10.6	10.0	2.0	27.6	0.20	2.76
Wire 5	10.6	10.0	2.0	36.8	0.20	3.68

superheated vapor state. Therefore, the thermodynamic properties at these locations can be determined based on the measured temperatures and pressures. The nitrogen was vaporized inside the test tube by the heat input. The exact heat input, including the heat input supplied by the DC power supply and the heat gain from the ambient, was estimated by using Eq. (1). The boiling heat transfer coefficients were determined by using Eq. (2). T_w in Eq. (2) was obtained by using the equation of steady-state radial heat conduction through the tube based on the measured outside wall temperatures. Vapor qualities of nitrogen were calculated by using Eq. (3)

$$Q = Q_{\text{heating}} + Q_{\text{gain}} = \dot{m}(i_{\text{out}} - i_{\text{in}}) \tag{1}$$

$$h = \frac{Q}{A(T_w - T_f)} \tag{2}$$

$$x(z) = \frac{i(z) - i_l}{i_{lv}} \tag{3}$$

The two-phase pressure drop of nitrogen inside the test tube was obtained by subtracting the single-phase vapor pressure drop from the total pressure drop measured as shown in Eq. (4). The total pressure drop was measured by using the differential pressure transducer installed between the inlet and outlet of the test tube. The single-phase vapor pressure drop was determined by using Eq. (5), and the length of the two-phase region in the test tube was calculated by Eq. (6). Two assumptions were made in these calculations: (1) the nitrogen at the inlet of the test tube was at saturated liquid state, and (2) the heat input to the test tube was provided at constant heat flux condition. The nitrogen entering into the test tube was maintained at slightly subcooled or saturated state by minimizing the heat gain to the connecting tube between the storage tank and the test tube by application of heavy insulations. The heat gain from the ambient can vary because the tube surface temperature increases along with the tube length. However, the vacuum insulation prevented any unbalanced heat gain across the whole tube length:

$$\Delta P_{\text{two-phase}} = \Delta P_{\text{total}} - \Delta P_{\text{single-phase}} \tag{4}$$

$$\Delta P_{\text{single-phase}} = (2 \times (l - l_{\text{two-phase}})(0.079 \times Re_v^{-0.25})G^2)/(\rho_v D) \tag{5}$$

$$l_{\text{two-phase}} = (\Delta i_{lv}/(i_{\text{out}} - i_{\text{in}})) \times l \tag{6}$$

The wire coil insert definitely enhanced the boiling heat transfer coefficient, but it also increased the pressure drop. Therefore, as shown in Eq. (7), the enhancement performance ratio (EPR) was introduced in the analysis of the test data to evaluate the performance of the wire coil inserts by considering both the heat transfer enhancement and pressure drop penalty [8]. Eqs. (8) and (9) show the heat transfer enhancement factor and the pressure drop ratio, respectively. As the EPR increases, the wire coil inserts become more effective:

$$\text{EPR} = \text{EF}/\text{PDR} \tag{7}$$

$$\text{EF} = h_{\text{en}}/h \tag{8}$$

$$\text{PDR} = \Delta P_{\text{en}}/\Delta P \tag{9}$$

3. Results and discussion

As shown in Fig. 4, the flow boiling data measured in this study are represented in the Steiner flow pattern map [9]. The flow patterns of the present tests are in the stratified or the stratified wavy flow region. As shown in Fig. 5, the upper and the bottom temperatures of the test tube also indicate stratified flow patterns. Before total dryout of the liquid film, the temperatures at the bottom side were very close to the saturation temperature of the nitrogen. However, the temperatures at the upper side were higher than those at the bottom side. Generally, the temperature difference between the upper and the bottom side decreased with the increase of the test section length at the

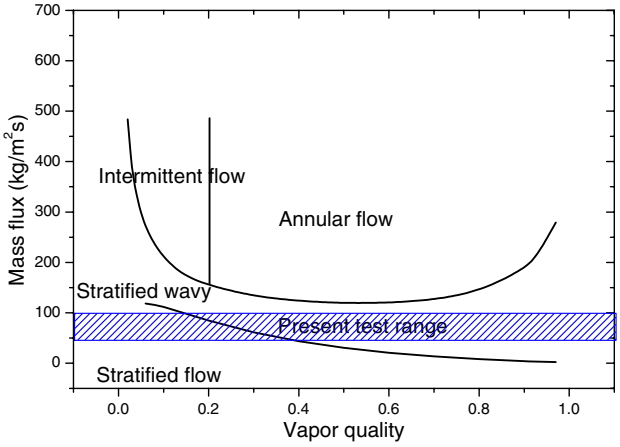

Fig. 4. Verification of the present flow patterns by using the Steiner flow pattern map.

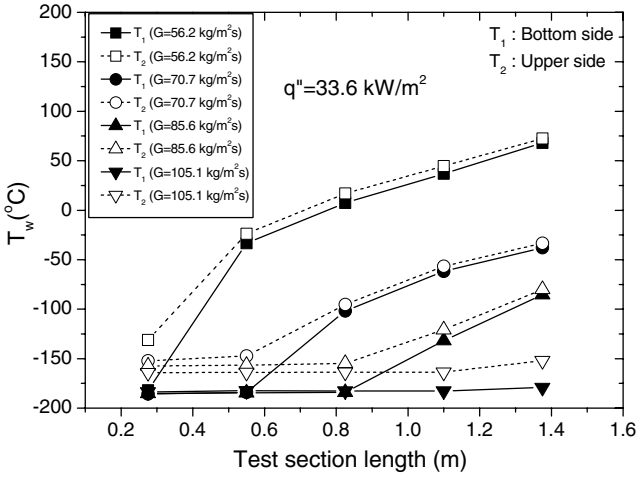

Fig. 5. Temperature profiles on the plain tube wall.

same mass flux. However, when the test length was less than 0.83 at the mass flux of 85.6 kg/m^2 s, the temperature difference was nearly constant at 28 °C due to the existence of the liquid film on the tube wall. The liquid film thickness on the tube wall decreased with the increase of the test tube length, and then finally the dryout occurred. The dryout point moved toward the inlet of the test section with the decrease of the mass flux at the same heat flux condition. At the mass flux of 105.1 kg/m^2 s, the stratified flow pattern without having total dryout was maintained along the whole length of the test section due to the thicker liquid film at the bottom side of the tube compared with that at the lower mass flux conditions.

Fig. 6 shows the heat transfer coefficients with vapor quality when mass flux varies from 56.2 to 105.1 kg/m^2 s at a heat flux of 33.6 kW/m^2. The heat transfer coefficients increase with the increase of mass flux. Fig. 6 also shows the comparison of the present data with the heat transfer coefficients predicted by existing correlations [10,11]. The Shah correlation [10] was one of the promising correlations for cryogenic fluids, even though it was developed based on the data of non-cryogenic fluids. The Hendricks et al. correlation [11] was developed for dispersed film boiling of cryogenic fluids. The present data were significantly lower than the predictions of the Shah correlation, while they were slightly higher than the data predicted by the Hendricks et al. correlation. This trend may be due to the partial wetting of the test tube by the liquid film during the boiling process of the nitrogen.

Fig. 7 shows the heat transfer coefficients for heat flux variation from 22.5 to 32.2 kW/m^2 at a mass flux of 70.7 kg/m^2 s. Generally, nucleate boiling is a dominant heat transfer mechanism at low vapor quality. In this region, the heat transfer coefficient was strongly dependent on heat flux, yielding higher values with the increase of heat flux. Under the stratified flow pattern, the liquid film deficient region around the tube wall enlarged with the increase of heat flux, resulting in the rapid drop of the heat transfer coefficient.

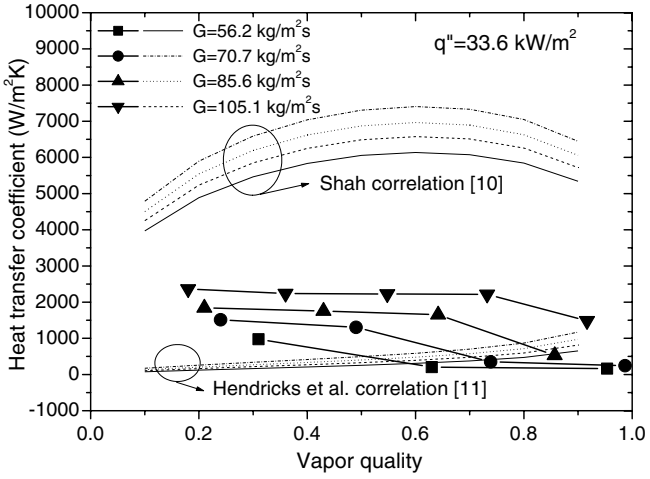

Fig. 6. Heat transfer coefficients with vapor quality for various mass fluxes.

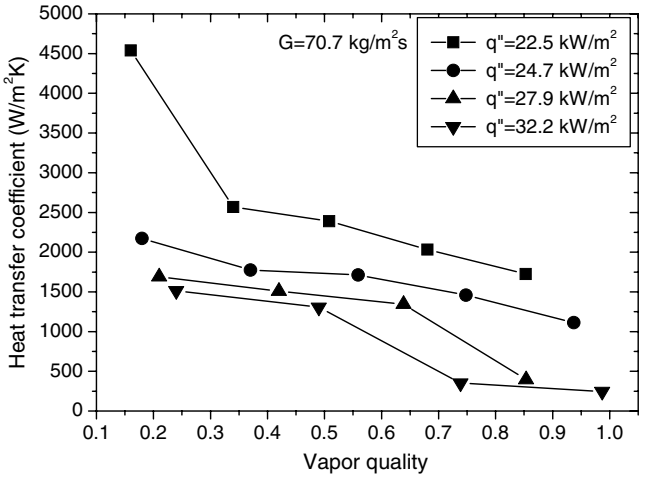

Fig. 7. Heat transfer coefficients with vapor quality for various heat fluxes.

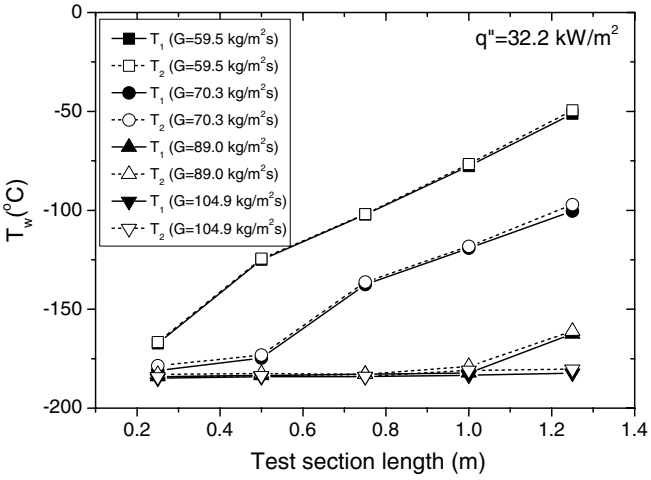

Fig. 8. Temperature profiles on the wire coil inserted tube wall.

Fig. 8 shows the temperatures at the upper and the bottom side of the wire coil inserted tube. The temperature difference between the upper and the bottom side of the tube was approximately 3 °C in the wire coil inserted tubes, which was considerably lower than that in the plain tube (Fig. 5). The temperature difference in the wire coil inserted tube may have reduced because of the swirl flow induced by the wire coil.

Fig. 9 shows the effects of the wire coil inserts having different wire thicknesses and a constant coil pitch of 18.4 mm. The heat transfer coefficients significantly increased with wire coil insertion into the tube. In addition, the heat transfer coefficients increased with the increase of the wire thickness. When the mass flux and heat flux were 104.9 kg/m^2 s and 34.1 kW/m^2, respectively, the average heat transfer coefficient of wire 3 ($t/D_w = 0.25$) was higher than that of the plain tube by 174%, while it was higher

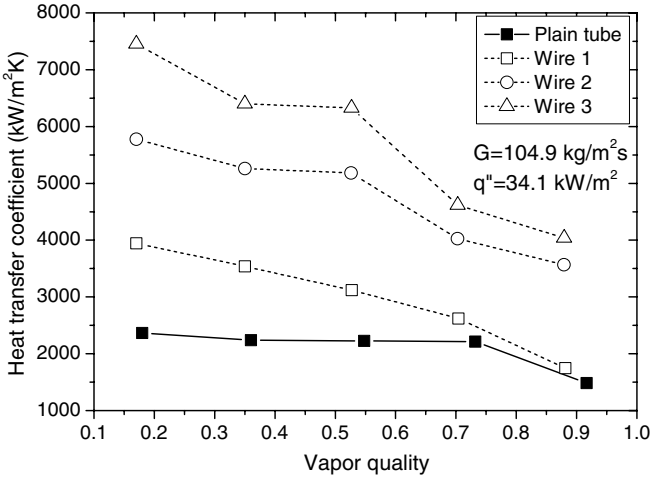

Fig. 9. Comparison of the heat transfer coefficients between the plain tube and the wire coil inserted tubes for various wire thicknesses.

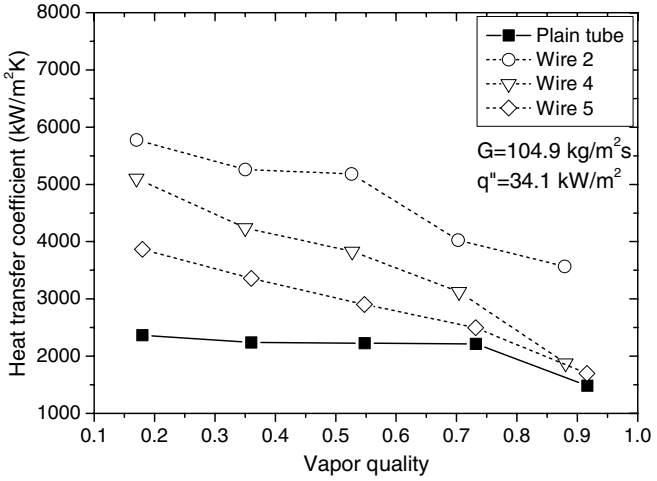

Fig. 10. Comparison of the heat transfer coefficients between the plain tube and the wire coil inserted tubes for various pitches.

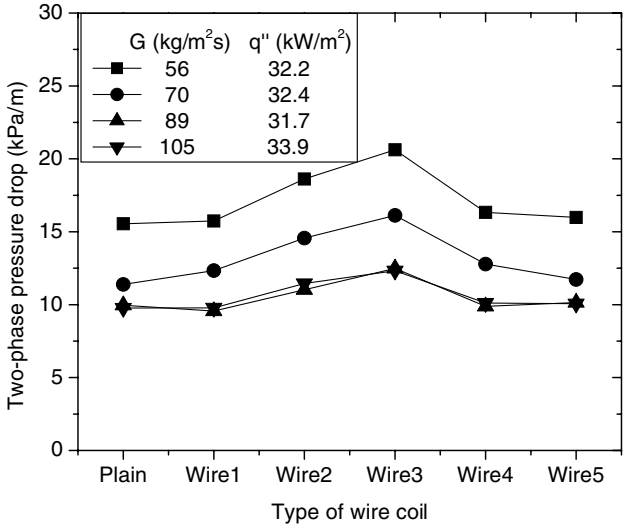

Fig. 11. Two-phase pressure drop of nitrogen for various wire coil inserts.

than those of wire 1 and wire 2 by 48% and 21%, respectively. The enhancement rate of the heat transfer coefficient in the wire coil inserted tube reduced with the increase of vapor quality. The swirl flow in the liquid film became more active with the increase of liquid film thickness, which yielded more heat transfer enhancement at low vapor quality because of the thicker liquid film thickness.

Fig. 10 shows the effects of the wire coil inserts having different pitches and a constant wire thickness of 2.0 mm on the enhancement of the heat transfer coefficients. The heat transfer coefficients increased with the reduction of the coil pitch. The heat transfer coefficients of wire 2 ($p/D_w = 1.84$) were higher than those of wire 4 and wire 5 by 23.7% and 40%, respectively. Table 2 shows the enhancement rate of the heat transfer coefficients by the wire coil inserts at various mass flux conditions. The heat transfer enhancement rate increased with the increase of mass flux. As the mass flux increased, the swirl flow became much stronger and the liquid film thickness at the bottom side of the tube increased. In addition, the dryout vapor quality increased with the increase of mass flux.

Fig. 11 shows the pressure drop of the plain and the wire coil inserted tubes. The pressure drop increased with the increase of wire thickness. The pressure drop of wire 3 was higher than those of wire 1 and wire 2 by 20.7% and 7.1%, respectively, at a mass flux of 105 kg/m^2 s. In addition, the pressure drop decreased with the increase of coil pitch. The pressure drop of wire 2 was higher than those of wire 4 and wire 5 by 11.7% and 12.1%, respectively, at a mass flux of 105 kg/m^2 s. On the other hand, the average pressure drop at a mass flux of 56 kg/m^2 s was 38% higher than that at a mass flux of 105 kg/m^2 s. The same trend was also reported by Steiner and Schlünder [12] for these mass and heat flux ranges. Lapin and Bauer [13] showed that the pressure drop of cryogenic fluids having the mist flow pattern was two times higher than that for the bubbly and the annular flow pattern. The possibility that the mist flow

Table 2
Heat transfer enhancement (%) by wire coil inserts

Wire coil no.	$G = 58.0$ kg/m^2 s	$G = 70.6$ kg/m^2 s	$G = 88.0$ kg/m^2 s	$G = 104.9$ kg/m^2 s
Wire 1	21.9	24.5	35.1	42.2
Wire 2	48.5	63.5	92.7	126.1
Wire 3	66.6	85.1	170.0	173.9
Wire 4	29.3	39.3	54.7	72.6
Wire 5	7.3	14.9	32.7	36.0

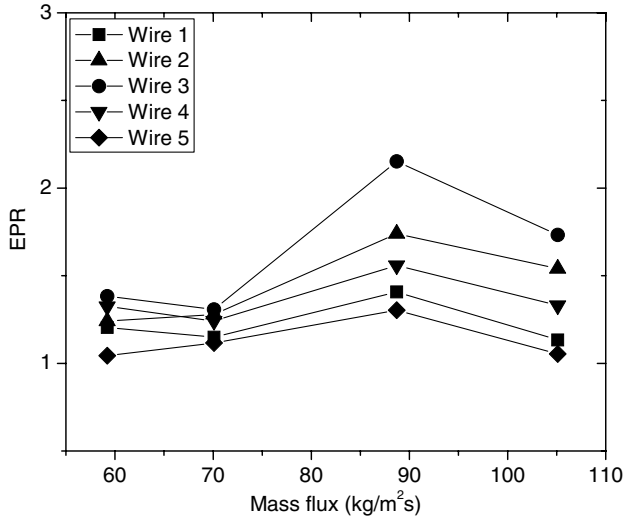

Fig. 12. Enhancement performance ratio with mass flux for wire coil inserted tubes.

would exist in the most part of the test tube under partial or total dryout conditions increased with the reduction of mass flux.

Fig. 12 shows the EPR with mass flux for the wire coil inserts. Generally, the heat transfer enhancement rate was relatively higher than the increase of the pressure drop. For the present test conditions, the EPR increased with the reduction of coil pitch and the rise of wire thickness.

4. Conclusions

The boiling heat transfer characteristics of nitrogen were experimentally investigated in a stainless steel plain tube and wire coil inserted tubes. The existence of the stratified flow under the present test conditions was predicted by the Steiner flow pattern map. The partial and total dryout of liquid film occurred in the flow boiling of nitrogen. The value of the heat transfer coefficient increased with the increase of mass flux, while it decreased with the increase of heat flux because the dryout vapor quality reduced with the increase of heat flux. The pressure drop increased with the reduction of mass flux. The probability on the existence of the mist flow under partial and total dryout conditions increased with the decrease of mass flux, resulting in a higher pressure drop. The wire coil insert induced swirl flow, which can force the liquid film at the bottom side to mix with the vapor at the upper side of the tube. Both the heat transfer coefficient and pressure drop increased with the reduction of the twist ratio p/D_w and the increase of the thickness ratio t/D_w. Wire 3 having a p/D_w of 1.84, and a t/D_w of 0.25 showed the best EPR among the tested wire coil inserts.

Acknowledgements

This work was supported by the Carbon Dioxide Reduction and Sequestration Center, one of the 21st Century Frontier R&D Programs in the Ministry of Science and Technology of Korea.

References

[1] H. Umekawa, M. Ozawa, Toshiaki Yano, Boiling two-phase heat transfer of LN_2 downward flow in pipe, Exp. Thermal Fluid Sci. 26 (2002) 627–633.
[2] H. Umekawa, M. Ozawa, Dryout and post-dryout heat transfer in a natural circulation loop of liquid nitrogen, Heat Transfer – Jpn. Res. 26 (1997) 449–458.
[3] X.L. Chen, W.H. Sutton, M.A. Sanchez, Film boiling of saturated nitrogen in horizontal tubes of double pipe heat exchangers, in: Proceedings of 10th International Conference on Nuclear Engineering, Arlington, VA, 2002, ICONE10-22777.
[4] W.F. Laverty, W.M. Rohsenow, Film boiling of saturated nitrogen flowing in a vertical tube, J. Heat Transfer 89 (1967) 90–98.
[5] K. Mori, K. Kasahara, Y. Shiota, H. Sonobe, S. Yamanoto, S. Takemura, A study on steam-heating LNG vaporizer, Mitsui Zosen Tech. Rev. 124 (1986) 37–43.
[6] S.C. Nam, S.C. Lee, B.D. Park, Performance of evaporation heat transfer enhancement and pressure drop for liquid nitrogen, J. Korean Soc. Mech. Eng. 24 (2000) 363–372.
[7] A.E. Bergles, W.D. Fuller, S.J. Hynek, Dispersed flow film boiling of nitrogen with swirl flow, Int. J. Heat Mass Transfer 14 (1971) 1343–1354.
[8] R.S. Reid, M.B. Pate, A.E. Bergles, A comparison of augmentation techniques during in-tube evaporation of R-113, J. Heat Transfer 113 (1991) 451–458.
[9] D. Steiner, Heat Transfer to Boiling Saturated Liquid, VDI-Wärmeatlas, Düsseldorf, Germany, 1993.
[10] M.M. Shah, Prediction of heat transfer during boiling of cryogenic fluids flowing in tubes, Cryogenics 24 (1984) 231–236.
[11] R.C. Hendricks, R.W. Graham, Y.Y. Hsu, R. Friedman, Experimental heat transfer and pressure drop of liquid hydrogen flowing through a heated tube, NASA TN D-765, 1961.
[12] D. Steiner, E.U. Schlünder, Heat transfer and pressure drop for boiling nitrogen flowing in a horizontal tube, Cryogenics 16 (1976) 387–398.
[13] A. Lapin, E. Bauer, Pressure drop of two-phase single component isothermal upward flow of nitrogen and methane at high pressures, in: K.D. Timmerhaus (Ed.), Advances in Cryogenic Engineering, vol. 12, Plenum, New York, 1967, pp. 409–418.